

See discussions, stats, and author profiles for this publication at: <https://www.researchgate.net/publication/351297108>

A Rapid Gamma-Ray Glow Flux Reduction Observed From 20 km Altitude

Article in *Journal of Geophysical Research Atmospheres* · April 2021

DOI: 10.1029/2020JD033467

CITATIONS

0

READS

10

14 authors, including:



Pavlo Kochkin

University of Bergen

41 PUBLICATIONS 371 CITATIONS

[SEE PROFILE](#)



David Sarria

University of Bergen

30 PUBLICATIONS 145 CITATIONS

[SEE PROFILE](#)



Nikolai G. Lehtinen

Stanford University

113 PUBLICATIONS 2,140 CITATIONS

[SEE PROFILE](#)



Andrew Mezentsev

33 PUBLICATIONS 177 CITATIONS

[SEE PROFILE](#)

Some of the authors of this publication are also working on these related projects:



ASIM Atmosphere-Space Interaction Monitor [View project](#)



Long Laboratory Sparks [View project](#)

JGR Atmospheres



RESEARCH ARTICLE

10.1029/2020JD033467

Key Points:

- A rapid reduction of a gamma-ray glow flux was observed from an aircraft at 20 km altitude
- The reduction happened synchronously with a lightning discharge beneath the aircraft and lasted for a few tens of milliseconds
- Spectral analysis of the weak and the strong glow fluxes do not suggest their different production mechanism

Supporting Information:

Supporting Information may be found in the online version of this article.

Correspondence to:

P. Kochkin,
pavlo.kochkin@uib.no

Citation:

Kochkin, P., Sarria, D., Lehtinen, N., Mezentsev, A., Yang, S., Genov, G., et al. (2021). A rapid gamma-ray glow flux reduction observed from 20 km altitude. *Journal of Geophysical Research: Atmospheres*, 126, e2020JD033467. <https://doi.org/10.1029/2020JD033467>

Received 13 JUL 2020

Accepted 15 APR 2021

Author Contributions:

Conceptualization: P. Kochkin

Data curation: S. Yang, G. Genov, K. Ullaland, M. Marisaldi, N. Østgaard, J. E. Grove, M. Quick, S. Al-Nussirat, E. Wulf

Formal analysis: P. Kochkin, D. Sarria

Funding acquisition: N. Østgaard, H. J. Christian, J. E. Grove

Investigation: P. Kochkin, D. Sarria, N. Lehtinen, G. Genov

Methodology: P. Kochkin, N. Lehtinen

Project Administration: N. Østgaard, H. J. Christian











Resources: S. Yang, G. Genov, K. Ullaland, N. Østgaard

Software: P. Kochkin

© 2021. The Authors.

This is an open access article under the terms of the [Creative Commons Attribution](https://creativecommons.org/licenses/by/4.0/) License, which permits use, distribution and reproduction in any medium, provided the original work is properly cited.

A Rapid Gamma-Ray Glow Flux Reduction Observed From 20 km Altitude

P. Kochkin¹ , D. Sarria¹ , N. Lehtinen¹ , A. Mezentsev¹ , S. Yang¹, G. Genov¹ , K. Ullaland¹ , M. Marisaldi¹ , N. Østgaard¹ , H. J. Christian², J. E. Grove³ , M. Quick⁴, S. Al-Nussirat², and E. Wulf³ 

¹Birkeland Centre for Space Science, University of Bergen, Bergen, Norway, ²University of Alabama, Huntsville, AL, USA, ³U.S. Naval Research Laboratory, Washington, D.C., USA, ⁴University of Maryland, College Park, MD, USA

Abstract Two gamma-ray glows were observed by a high-altitude NASA ER-2 aircraft flying at 20 km altitude over a thunderstorm in Colorado, USA. The flux of the first glow rapidly intensified and then abruptly decreased within a few tens of milliseconds. On a timescale of seconds, the flux decrease occurred simultaneously with a hybrid intra-cloud/cloud-to-ground lightning discharge beneath the aircraft. However, a more detailed analysis of the discharge dynamics indicated that the discharge activity was unusually calm during the actual period of the flux decrease. The lightning was observed with on-board antennas, optical sensor, and ground-based lightning mapping and location networks. Its closest activity was 12 km away from the aircraft, below and slightly ahead the course. The gamma-ray flux reduction happened roughly in the middle of the lightning development process. The glow spectral analysis for the periods of a weak and strong flux enhancement has been done. The spectra were found to be background-like and similar to each other.

1. Introduction

A long-duration gamma-ray emission from storm clouds, also referred as gamma-ray glows, were for the first time observed in 1981 (Parks et al., 1981). They last from sub-seconds to minutes and presumably generated by high electric fields of thunderclouds. Glows were observed both, initiated and terminated by lightning discharges (Eack, 1996). Besides interest for aviation safety, they can provide possibilities to study Relativistic Runaway Electron Avalanche (RREA) process in nature. Many experimental and theoretical works are focused on how glows are produced, but only a few on how they are terminated.

In 1980s, a NASA F-106 jet flew through many thunderstorms with a gamma-ray detector on-board (Parks et al., 1981). Several long-lasting gamma-ray flux enhancements were detected. One was reported to be terminated 0.1 s prior to a lightning flash (McCarthy & Parks, 1985). Electric-field measurements were not available and the flash initiation moment was identified by an optical sensor. However, since the aircraft was flying directly through the electrified cloud, it is possible that the lightning flash was triggered by the aircraft itself and eventually terminated the glow.

Later, Eack et al. conducted a series of balloon observations. The balloons were equipped with gamma-ray detectors and an electric field probe; they were launched into active thunderstorm systems (Eack, 1996; Eack et al., 1996a, 1996b, 2000; Eack & Beasley, 2015). The observation confirmed that the glow termination is associated with a lightning discharge. The instrument sampling rate was 250 ms, therefore could not provide more information on the termination dynamic. In later campaigns, the instrument resolution was increased to 66 μ s (15 kHz), but no results on glow termination moment were reported.

The Airborne Detector for Energetic Lightning Emissions (ADELE) observed 12 gamma-ray glows, one of them was abruptly terminated presumably by a lightning flash (Kelley et al., 2015). Unfortunately, the electric field data were not available and the flash itself was not detected.

The gamma-ray glow termination process was also observed from the ground (Tsuchiya et al., 2013). The gamma-ray flux increase collapsed 800 ms prior to a lightning flash. The flash was again not detected by any ground-based lightning location networks, but was identified in local instrument electric field antenna and optical sensor data (not shown in the paper). The gamma-ray time resolution was as good as 100 ms, however the lightning moment was given with 1 s accuracy only.

Supervision: N. Østgaard

Validation: P. Kochkin, N. Lehtinen

Visualization: P. Kochkin, D. Sarria

Writing – original draft: P. Kochkin

Writing – review & editing: P.

Kochkin, D. Sarria, N. Østgaard

Another observation was recently reported in Kochkin et al. (2017). Two gamma-ray detectors flew on-board of an A340 aircraft as a part of the In-flight Lightning Damage Assessment System (ILDAS). A 20-fold increase over the background count rate was observed near a thundercloud. The increase collapsed to background level before a discharge signature had been detected by an on-board electric field antenna. It was then hypothesized that the gamma-ray glow was not terminated by a lightning flash, but rather collapsed and initiated the flash.

In 2016, the ILDAS campaign detected positron annihilation signal in association with electrostatic discharges from an aircraft (Kochkin et al., 2018). The aircraft was flying through a gamma-ray glow region in proximity of a strong convection core of a thundercloud. Similar observation under similar circumstances was for the first time reported in Dwyer et al. (2015). So far the phenomenon lacks complete understanding.

Two most recent observations of the glow termination moment are reported from Japan. In Wada et al. (2018), the glow was observed from the ground using gamma-ray detectors synchronized with DC electric field and low frequency antenna measurements. Authors demonstrated that the glow was terminated by a lightning flash initiated 15 km away from the observation site. The glow was terminated at the moment when the flash was passing over the gamma-ray detectors. In Wada et al. (2019), the glow termination was observed synchronously with a lightning discharge and a downward Terrestrial Gamma-Ray Flash (TGF). Although both phenomena, the glow and the TGF, are probably produced by the same RREA mechanism, the precise relation between them is still unclear and is of high scientific attention.

Apparently, the gamma-ray glows are produced by the Modification Of the energy Spectra (MOS) mechanism in weaker electric fields (Chilingarian et al., 2010, 2012), and by the RREAs in stronger fields. In either way, they are found during the initial phase of a particle acceleration in thundercloud electric fields. But do two different production mechanisms imply different termination dynamic? Understanding the gamma-ray glow dynamics is crucial for connecting the glows with other high-energy emissions originated in thunderclouds.

In this work, we report on two gamma-ray glows with the focus on a flux reduction moment. The glows were observed from an aircraft at 20 km altitudes, 7 km above the thundercloud top. The flux was reduced by a hybrid intra-cloud/cloud-to-ground (IC/CG) lightning discharge shortly after its rapid intensification. We analyze the glow spectra for possible indication of their production mechanism. This paper is an accompanying paper to Østgaard et al. (2019) where the gamma-ray glows were reported and modeled. Here, we focus on the termination moment of the glow and analysis of the lightning flash that caused the termination.

2. Instrument and Data

In the present analysis, the data from the on-board instruments and ground-based lightning location networks have been used. The Airborne Lightning Observatory for FEGS and TGFs (ALOFT) is an aircraft-based experimental platform dedicated to studying lightning and its related phenomena. The acronym FEGS stands for the Fly's Eye Global lightning mapper Simulator. The platform is deployed on a NASA ER-2 high-altitude aircraft and contains, among others, two gamma-ray instruments, an Electric Field Change Meter (EFCM), an optical lightning mapper, and a Cloud Physics Lidar (CPL). The EFCM and the gamma-ray detectors are located inside the right pod as shown in Figure 1. The EFCM is a flat-plate antenna which is pointed straight ahead.

2.1. On-Board Instruments

The gamma-ray detector contains three bismuth germanate (BGO) crystals attached to photomultipliers and sealed in an aluminum container. One BGO crystal dimensions are $150 \times 50 \times 32$ mm. The detectors were calibrated before the campaign using various calibration sources and the muon peak. They are sensitive to photons in 0.1–40 MeV energy range. The data acquisition system has a 27 ns digital sampling rate and allows for storing information about each individual count during the entire flight. The data are downloaded from the on-board computer and analyzed after landing. The data acquisition system is similar to the one used in the Atmospheric Space Interaction Monitor (ASIM) mission and thoroughly described in Østgaard et al. (2019). The system has an intrinsic ability to identify the detector's saturation when subsequent



Figure 1. The ER-2 Airborne Lightning Observatory for FECS and TGFs (ALOFT). The electric field change meter (EFCM) and the gamma-ray detectors (BGO) are located inside the right pod. The image is from (Tatum, 2017). ALOFT, Airborne Lightning Observatory for FECS and TGFs; BGO, bismuth germanate; EFCM, electric field change meter; FECS, Fly's Eye Global lightning mapper Simulator; TGF, Terrestrial Gamma-Ray Flash.

counts start overlapping. The saturation has not been observed during the reported campaign, therefore no “dead-time” effects are present in the data. The data contain timestamps from a GPS receiver and have absolute timing uncertainty of several tens of nanoseconds.

The EFCM was a part of another experimental campaign. It consists of two annulus antennas separated from a ground plate by insulating standoffs. Unfortunately, we do not have sufficient understanding of the instrument bandwidth besides “fast” and “slow.” The signal from the antennas has GPS timestamps. The data from the low-frequency “slow” antenna were used to identify the moment of the charge transfer. The data from the high-frequency “fast” antenna were compared against data from a lightning mapping array and ground based lightning location networks. The EFCM data considered as supplementary in the analysis.

The main payload of the aircraft was the FECS optical instrument (Quick et al., 2015). It contains 30 radiometers organized in a pattern that monitors roughly a square 10×10 km area at the cloud top altitude under the aircraft. The data can be downloaded from the FECS data set Quick et al. (2019). The data set consists of lightning flash, lightning pulse, and radiance data collected by the optical instrument in GOES-R Post Launch Test (PLT) airborne science field campaign.

The CPL (McGill et al., 2002) was also installed on-board of the aircraft. The purpose of the CPL is to provide multi-wavelength measurements of cirrus, sub-visual cirrus, and aerosols with high temporal and spatial resolution. Cloud profiling provided cloud location and an internal backscatter structure with 30 m vertical and 200 m horizontal resolution. In this study, the CPL was used to reconstruct the cloud top height (CTH) with higher resolution than available from the Geostationary Operational Environmental Satellite (GOES) Imager.

2.2. Ground-Based Instruments

The Colorado Lightning Mapping Array (COLMA) provided their data for the region (Stano et al., 2014). There were 15 stations active during the observation day. The distance from the array center to the observation site was 140 km. The array provides information about the very high frequency (VHF) source latitude, longitude, altitude, reduced chi-square, and power. The sources with the chi-square lower than 5 were used in the present analysis.

The Earth Networks Total Lightning Network (ENTLN) data were used for the analysis of the lightning activity in the region. ENTLN is a lightning detection network with more than 1,200 sensors deployed globally.

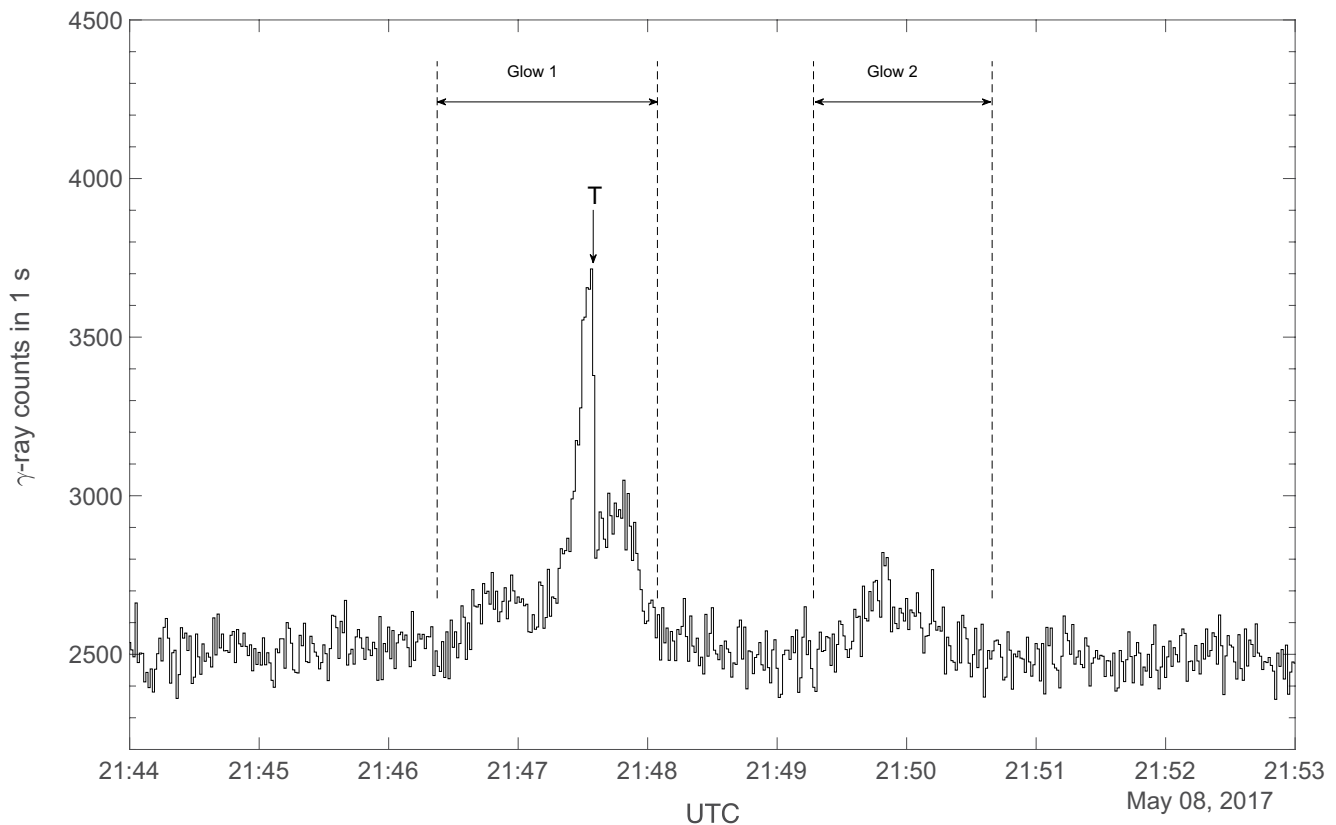


Figure 2. The gamma-ray count rate measured at 20 km altitudes over a thundercloud binned in 1 s intervals. Two gamma-ray glows are indicated. The first glow is abruptly reduced at the moment T, shortly after a sudden increase of its intensity. The peak intensity is 46% higher than the characteristic background at the altitude.

The ENTLN is capable of detecting the components of both IC and CG flashes. More on its performance can be found in Rudlosky (2015); Zhu et al. (2017); Marchand et al. (2019). The World Wide Lightning Location Network (WWLLN) data are included in the ENTLN database and were also used in the analysis.

3. Observation

On May 8, 2017, the ER-2 approached a thunderstorm from the East side of Colorado, USA, with the speed of 210 m/s at the cruise altitude of 20 km. Figure 2 shows a 1-s binned gamma-ray count rate for the selected period. Two gamma-ray glows were detected. The background count rate was at the level of $R_{bg} = 2,500 \pm 50$ cps, characteristic for this altitude. At 21:46:30 UTC, the count rate started to increase. After about 45 s of gradual increase, which corresponds to 10 km traveled distance, it reached 2,650 cps (6% increase) and then suddenly intensified. In 30 s, the count rate reached the highest detected level of $R_{max} = 3,650$ cps, which is 46% increase over the background. At this moment, it was abruptly reduced down to 2,900 cps, and then gradually to the initial background level. The maximal detected flux from the source presumably located beneath the aircraft was therefore $F_{source} = (R_{max} - R_{bg})/A_{BGO} = 1,150(\text{cps})/225(\text{cm}^2) \approx 5 \text{ cps/cm}^2$. Here, A_{BGO} is the geometric area of the gamma-ray detector. The total duration of the gamma-ray glow was 100 s, which corresponds to 20.6 km traveled distance.

One minute after the first glow, the gamma-ray flux increased for the second time. This glow was only 10% above the background level. It lasted for 80 s, which corresponds to 18.4 km traveled distance. The flux was again reduced at the peak moment, also with an associated lightning discharge. But this event was not intense enough for the termination moment analysis.

The gamma-ray glows were considered in detail in Østgaard et al. (2019). The thundercloud system where the glows originated from had a strong convection core. The glows were found in the direct vicinity of

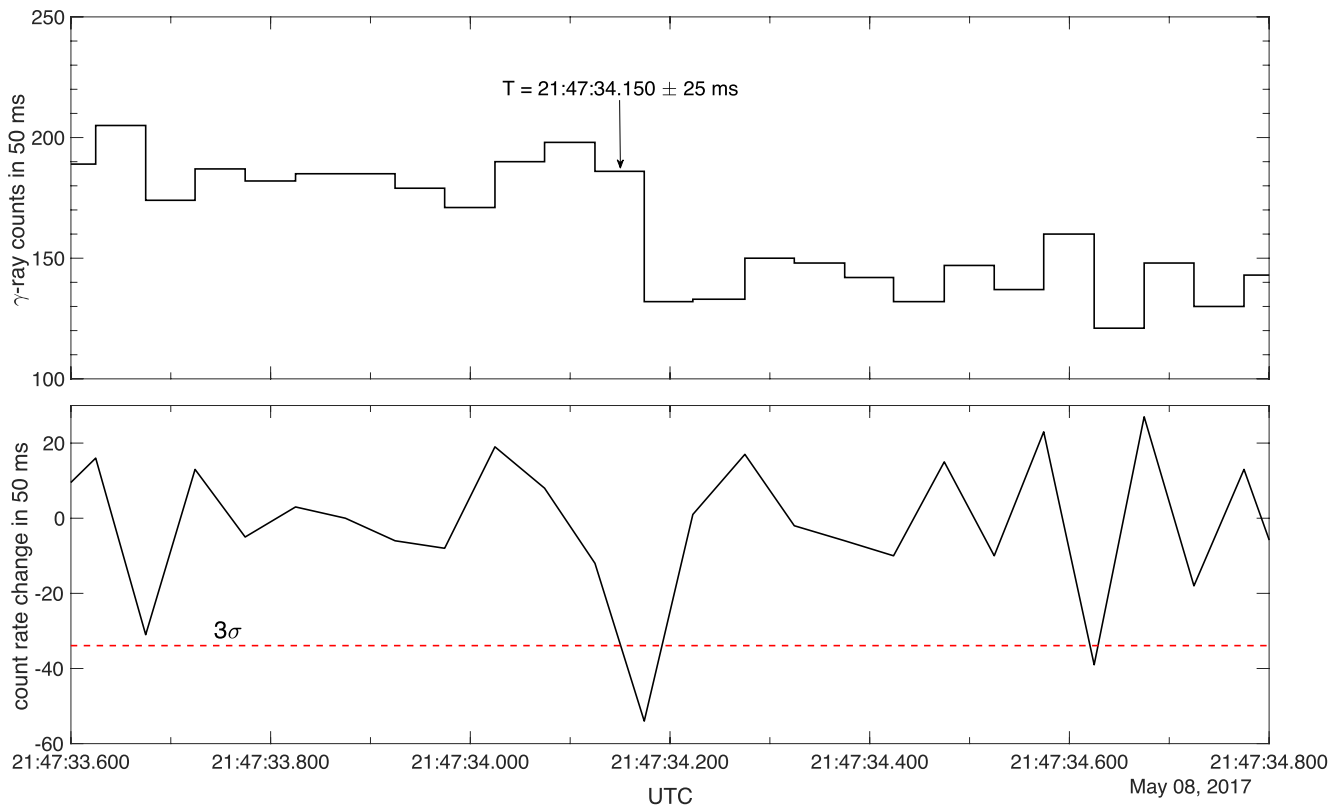


Figure 3. The glow reduction time is determined by the running difference between subsequent bins. When the difference exceeds 3σ for the applied binning, the reduction moment is set to the bin center with a half-bin margin. The reduction moment is identified at $T = 21:47:34.150 \pm 25 \text{ UT}$.

the core. The on-board electric field measurement combined with the radar and COLMA data suggest an inverted charge structure of the thundercloud. The inverted charge structure implies an upper negative charge layer with a lower positive charge layer below it. Modeling results indicated two possible production mechanisms for the glows, an enhancement of the cosmic background locally and a RREA inside the cloud. However, it is not clear how the inverted charge structure can produce such intense glow in a backward direction. A similar polarity problem is reported in Wada et al. (2018) for a glow observed from the ground.

3.1. The Reduction Time

To identify the reduction moment, the incremental re-binning method was applied. In the first step, the gamma-ray count rate is binned with 10 ms bin size. The average standard deviation $\langle\sigma\rangle$ is estimated for the 10 min period centered on the glow. Then a count rate change is calculated by running difference between two subsequent bins. If the count rate change does not exceed $3\langle\sigma\rangle$ near the reduction moment, the bin size is increased and the procedure is repeated from the first step. The reduction time is then assigned to the bin where the count rate change has dropped by $3\langle\sigma\rangle$. The bin's central time is chosen for the reduction moment with a half-bin margin on both sides. It was found that the optimal (confident) bin size is 50 ms and the reduction moment is identified at $T = 21:47:34.150 \pm 25 \text{ ms UT}$. Figure 3 shows the count rate change with 50 ms bin size. During the 50 ms centered around T , the gamma-ray count rate has reduced from 186 counts to 132, which is 29% or $4.8\langle\sigma\rangle$.

As any physical process, the flux reduction moment has a duration. Figure 4 shows the count rate in 10 ms bins using different initial bin timestamp. While the signal is very noisy with such a small bin size, the bottom three panels may indicate a gradual decay of the count rate. The top two panels, on the other hand, cannot be interpreted as a decay. Therefore, it is safe to conclude that the glow reduction moment lasted no longer than a few tens of milliseconds.

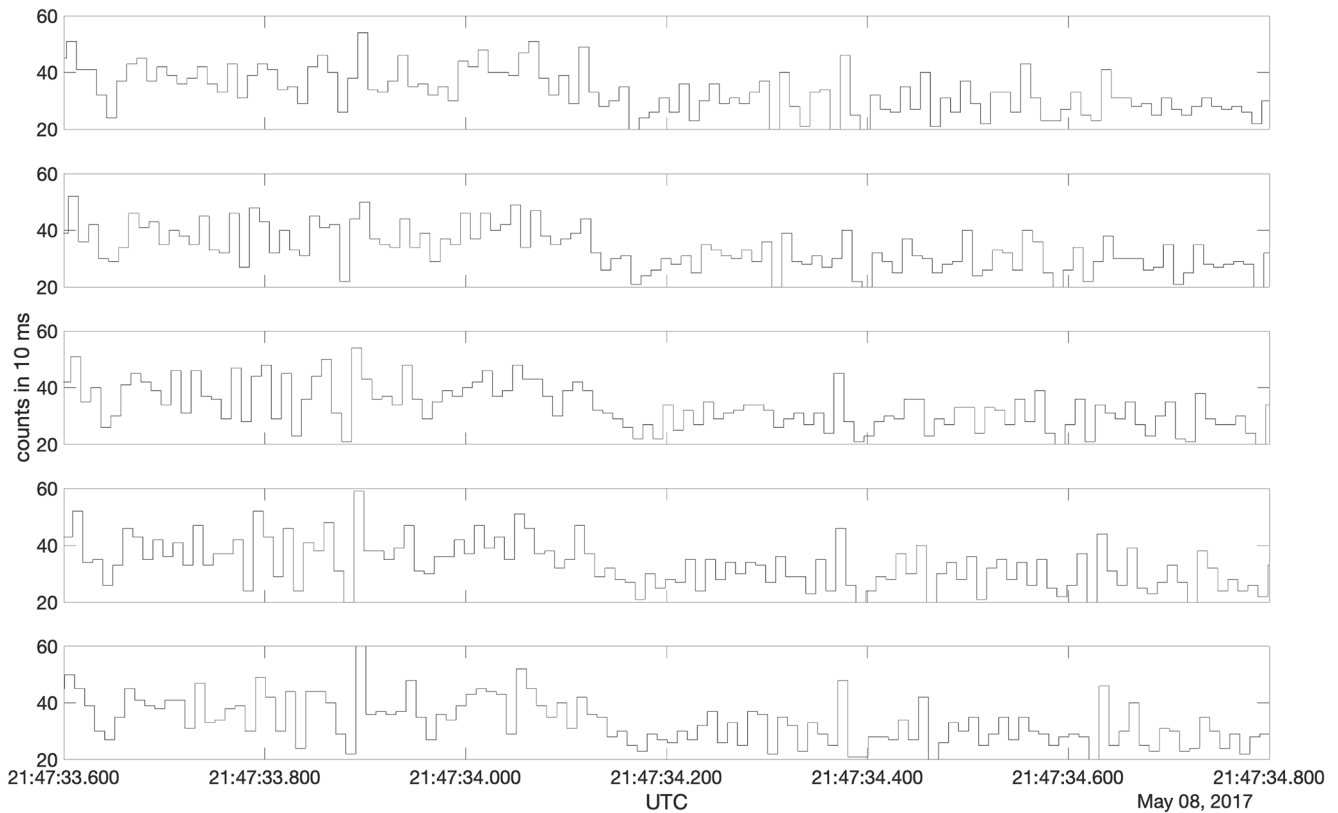


Figure 4. The gamma-ray count rate binned in 10 ms. Some of the panels (3–5) show slight indication of a gradual decay, while the others (1 and 2) can be interpreted as abrupt.

3.2. The Reduction Region

Figure 5 shows the cloud top height, the aircraft trajectory and the COLMA VHF sources for ± 0.5 s around the flux reduction moment T . The aircraft moves from the East (right) to the West (left).

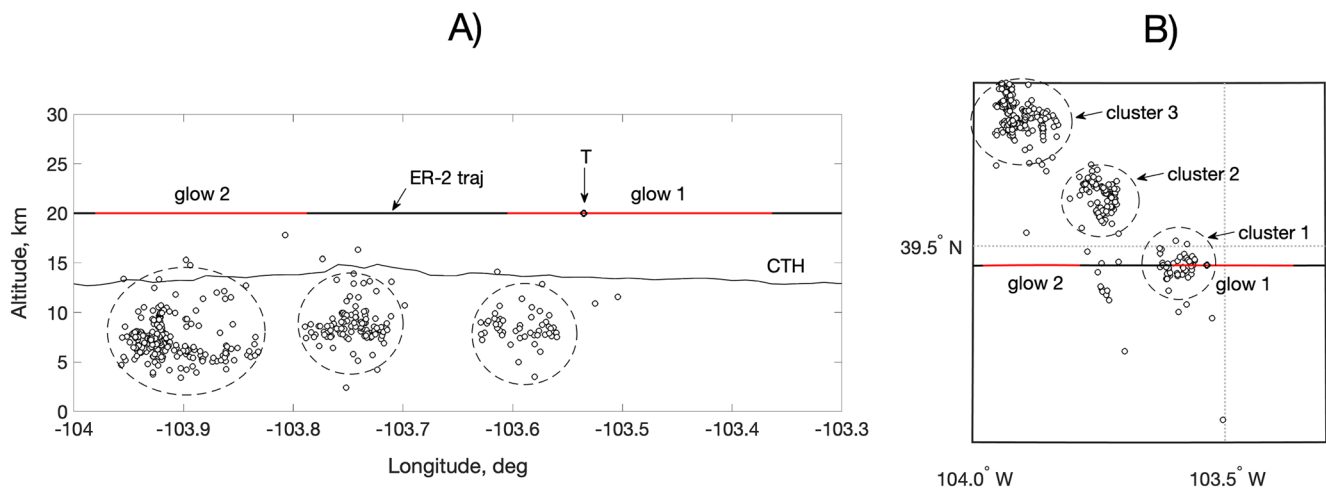


Figure 5. The ER-2 flight trajectory at 20 km altitude during the glow observation. (a) The altitude versus longitude projection. The Cloud Top Height (CTH) as recorded by the LIDAR is indicated. Two regions when gamma-ray glows were detected are marked with red lines. The glow reduction moment is marked by the arrow with a “T” label. The COLMA VHF sources from the half-second before to the half-second after the T-moment are plotted as small circles. The sources constitute three distinct clusters. (b) The same as above but in conventional geographic map projection. COLMA, Colorado Lightning Mapping Array; CTH, Cloud Top Height; VHF, very high frequency.

Table 1
The COLMA VHF Source Cluster Size and Distance to the Aircraft at the Moment of the Glow Flux Reduction

S	Cluster 1	Cluster 2	Cluster 3
Distance to aircraft, km	12.5	22.0	42.0
Diameter, km	6	7	8

Abbreviations: COLMA, Colorado Lightning Mapping Array; VHF, very high frequency.

apex reached 14.9 km, as measured by the LIDAR on-board the aircraft. Three distinct clusters of COLMA sources can be seen during this time. The activity in cluster 1 lasted for 340 ms, the sources are closest to the aircraft and originated roughly from a sphere of 6 km diameter located 8.6 ± 1.2 km above the sea level. The distance from the aircraft to the sphere center is 12.5 km. The center location of the cluster is determined as the mean value of its (latitude, longitude, and altitude) coordinates. The diameter of the cluster is determined as a sphere containing 95% of the sources. Table 1 shows the size and the distance from the aircraft to the three clusters.

Figure 6 shows the lightning activity in three clusters in the LMA format. The aircraft trajectory, glow regions, and the aircraft position at the glow flux reduction moment are shown. Despite the clusters appear spatially isolated, the timeline of the lightning activity indicates that they are parts of the same extensive hybrid IC/CG lightning. The lightning begins with two IC strokes in cluster 2 and 3 (dark-blue squares), then it develops into two negative CG strokes in the same clusters (dark-blue triangles), and then the discharge continues propagating to cluster 1 where it ends as an IC stroke (brown square). The CG peak currents are -13 and -8 kA in cluster 2 and 3, respectively. Remarkably, they did not reduce the glow intensity. The glow flux reduction moment T is shown as a vertical solid black line on the top panel of the figure. On the timescale, the reduction moment is situated between two IC discharges in cluster 3, but it clearly happens only after the lightning reaches the charge region associated with the cluster 1.

Figure 7 shows lightning activity in three clusters near the gamma-ray flux reduction moment side-by-side. Cluster 1 has discharge activity before and after the reduction moment. Remarkably, it contains a period with no VHF sources exactly during the identified time slot when the flux has rapidly dropped. Cluster 2 has a strong lightning activity right before the reduction moment T and almost nothing after it. Cluster 3 has a strong VHF source activity long before, during, and after the reduction moment. The activity in cluster 3 is intensified right after the T. All three clusters are located inside the EFCM direction beam, hence can be seen by the on-board antennas. Only the cluster 1 was seen in the optical FECS instrument.

Figure 8 top panel shows the gamma-ray count in 50 ms bins versus time and COLMA sources from cluster 1. Both WWLLN and ENTLN reported a lightning stroke synchronously with the last COLMA source from the same region. ENTLN identified it as an IC negative discharge with $-5,420$ A peak current. This is consistent with the on-board slow antenna measurement.

Middle panel: the fast and slow antenna electric field measurements and optical power from cluster 1. Bottom panel: the source altitude versus time plot. Black dots were reconstructed from the fast antenna measurements. The squares are the COLMA VHF sources.

The middle panel of Figure 8 shows the slow and the fast antenna E-field measurements and optical power from one radiometer of the FECS optical instrument. The E-field data were obtained in 1 s intervals in triggered mode. The radiometer is pointed toward the cluster 1.

The slow antenna detected a significant charge motion before and after the gamma-ray flux reduction. Positive signal implies that negative charge moves away from the aircraft. The signal shows a rising slope followed by a nearly flat region and followed by another rising slope until it peaks. The flat region coincides with the identified glow flux reduction period.

The following remarkable observations are worth mentioning.

- The trail of the optical pulses at the end of the flash starting at 21:47:34.27 is almost entirely missed by all ground-based networks. Only one optical pulse in the middle of the trail was detected by COLMA, WWLLN, and ENTLN simultaneously. We attribute the optical pulses to recoil processes
- The intense trail of COLMA VHF sources right after the T-moment are located between two large optical pulses at 21:47:34.17 and 21:47:34.27 and are accompanied by a nearly constant level of optical emission. The period corresponds to a negative leader progression in cluster 1

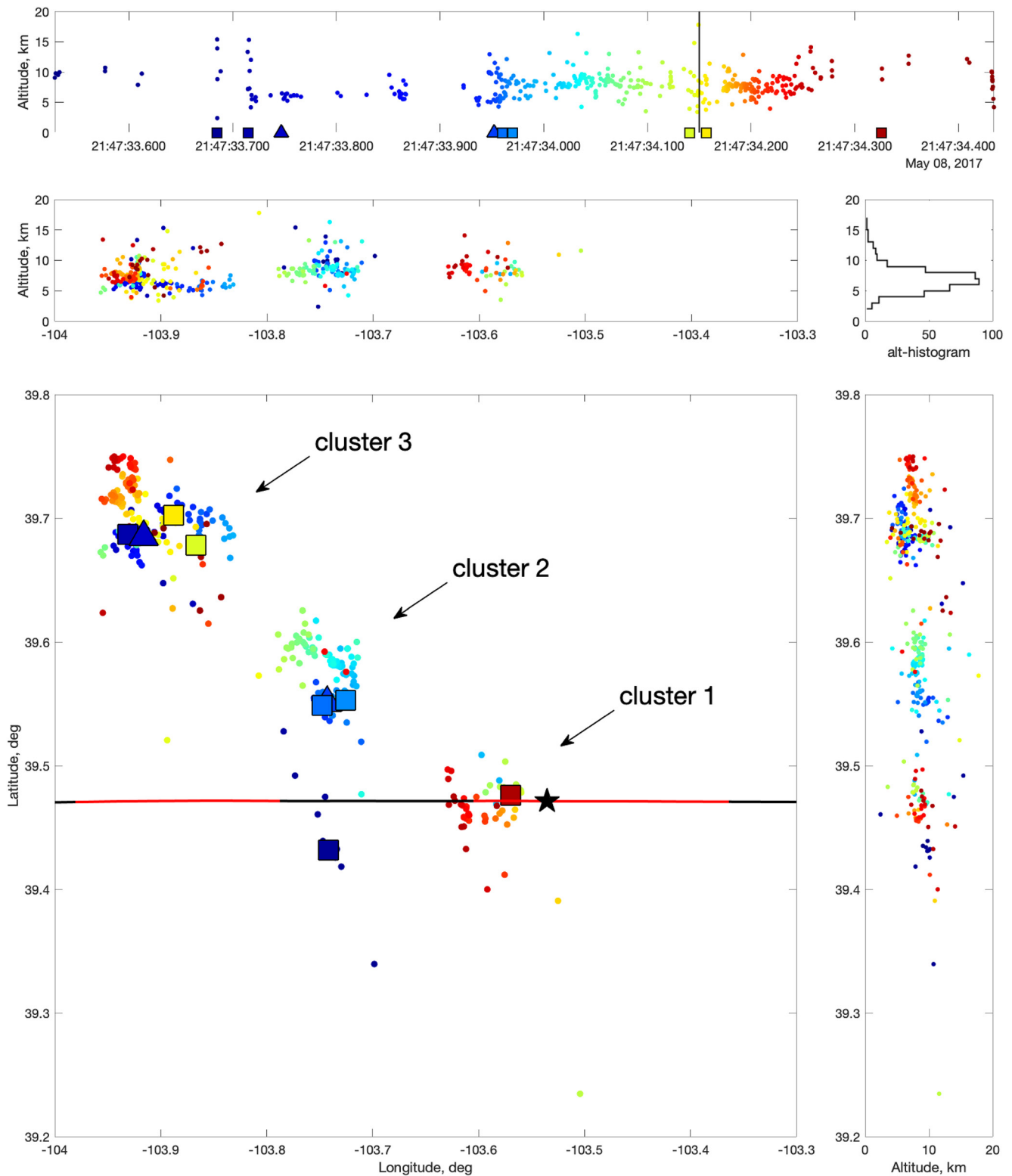


Figure 6. The temporal and spatial locations of the VHF sources are plotted and color-coded. The aircraft trajectory is shown as the horizontal solid black line on the longitude versus latitude projection. The gamma-ray glow regions are marked in red on the trajectory line. The aircraft position at the flux reduction moment is indicated with a star. The glow reduction time is shown as a vertical solid line on the top panel. The ENTLN negative cloud-to-ground strokes are shown as triangles, the intra-cloud strokes are shown as squares. ENTLN, Earth Networks Total Lightning Network; VHF, very high frequency.

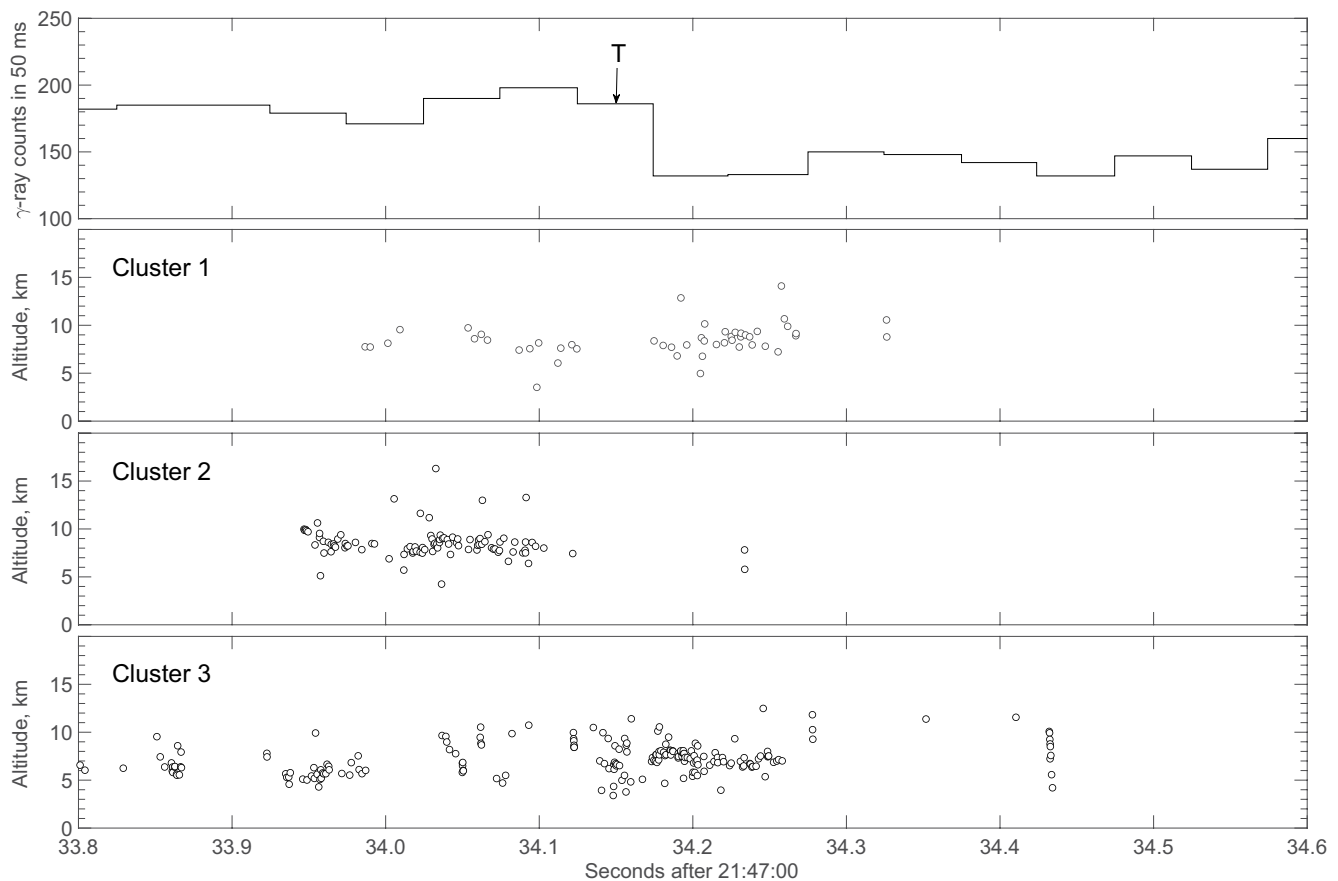


Figure 7. Top panel: The BGO gamma-ray count rate in 50 ms bins. The three bottom panels show lightning activity in three clusters during the gamma-ray glow flux reduction moment. BGO, bismuth germanate.

- The 50 ms period during the glow flux reduction shows a gradually increasing level of optical activity with a small pulse in the middle at 21:47:34.14. The pulse is missed by COLMA but can be seen in the HF antenna. We tentatively attribute this period to a positive leader progression in cluster 1

The slow baseline variation in the optical signal during the flux reduction period may well be attributed to the aircraft motion while the optical sensor scans the field of view. We base our assumption about the positive leader propagation during this period on two remarks: (1) there is some electrical activity during this period that is apparent from the two optical pulses (still might be scattered light) and (2) the propagation of the negative leader immediately after the period is also detected as a slow baseline variation.

4. Spectral Analysis

Overall, the observation contains periods of weak flux enhancements and one period of a strong flux increase. The strong flux increase is observed in the middle of the weaker enhancements. We speculate that such structure could be explained by the assumption that the weak enhancements are produced by the MOS mechanism (electric field below the break-even field) and the period with the strong flux is produced by the RREA process that requires stronger fields. MOS can only account for a few percent flux increase with a similar to background spectrum, while RREA can multiply the initial flux some orders of magnitude but has a characteristic 7–8 MeV exponential cut-off energy. The fact that the strong flux enhancement was not completely terminated by the lightning but dropped to the level of the weaker glow may also indicate that the phenomena are spatially separated. Interestingly, the spectra of both, the weak and the strong enhancements, look very similar to each other and to the background. Figure 9 shows the spectra of the weak and strong glows.

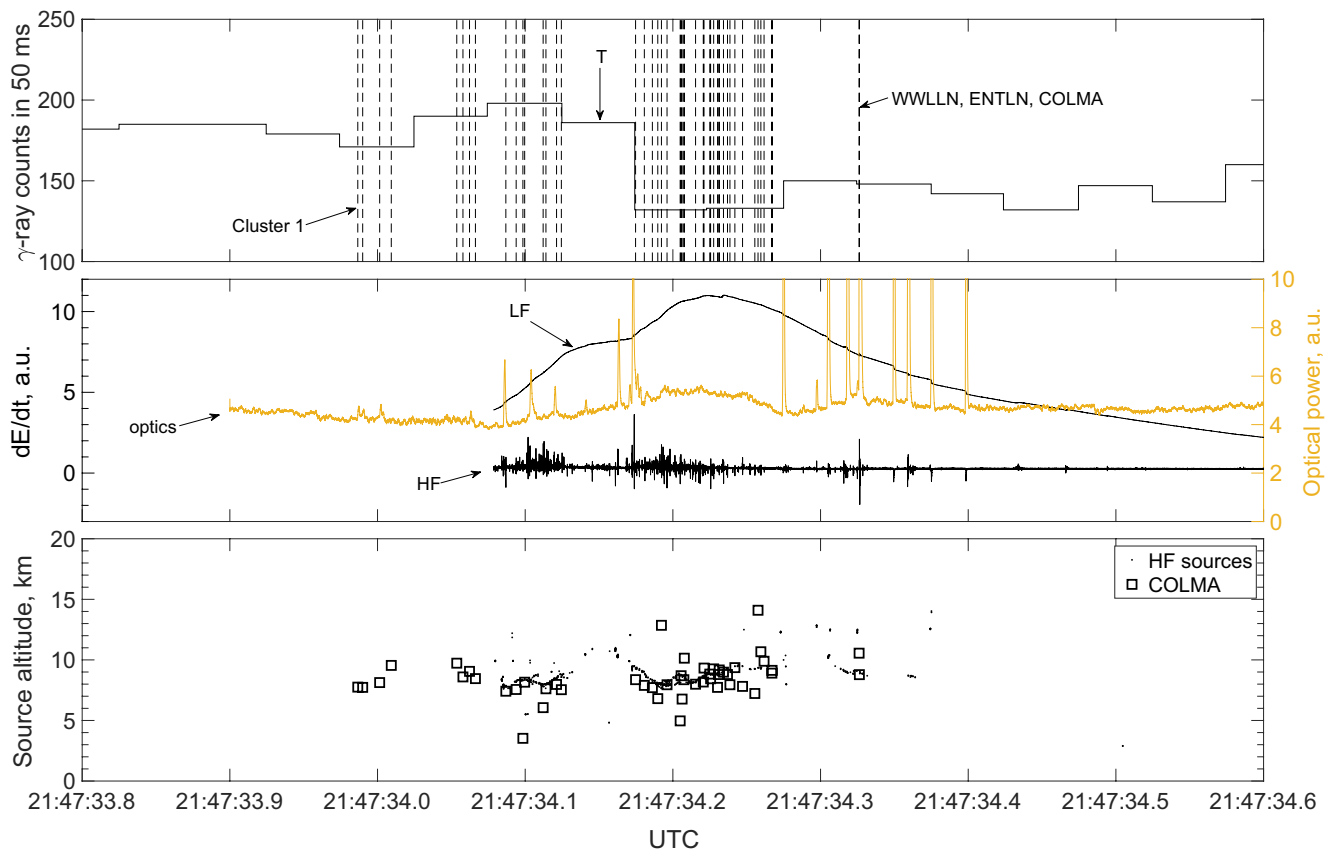


Figure 8. Top panel: the photon count rate in 50 ms bins. The cluster 1 timestamps of the encircled sferics from Figure 5 are shown as vertical dashed lines. The last VHF-source of the COLMA flash was also detected by ENTLN and WWLLN. COLMA, Colorado Lightning Mapping Array; ENTLN, Earth Networks Total Lightning Network; WWLLN, World Wide Lightning Location Network.

For the weak glow spectra, the counts during 73 s have been accumulated from around the strong flux increase. The total number of counts is 205,640, among which roughly 190,000 are from the background. For the strong glow, the total number of counts in the spectra is 61,533 collected over 19 s, among which 50,000 are from the background. The glow spectra are background-subtracted and normalized on the total intensity and duration. The one-sigma error bars are shown in assumption of Poisson counting statistics. The background uncertainty is added to the signal uncertainty in quadrature.

Both, the weak and the strong glows, have similar to background spectra with missing high-energy part. The high-energy peak in the background spectra at around 30 MeV is caused by muons with energies above several GeV that hit the detector from above. As expected, the peak is missing in the glow spectra. There is an intriguing discrepancy between the weak and the strong glows in 8–10 MeV range, where the strong glow has more counts than the weak one. However, in the MOS and RREA interpretation, it is expected that the weaker glow should have more counts in this energy range instead of the strong one. The spectra are remarkably similar in the other energy bins, therefore, we avoid making strong claims on the discrepancy. More on the spectra and effort to understand the origin of the emission can be found in Østgaard et al. (2019).

5. Discussion and Conclusions

In this work, we analyzed a gamma-ray glow flux reduction moment. The analysis was performed on a 50 ms timescale, which was estimated to be the most suitable for the study. The reduction moment itself lasted for no more than a few tens of milliseconds. Three clusters of high lightning activity were identified

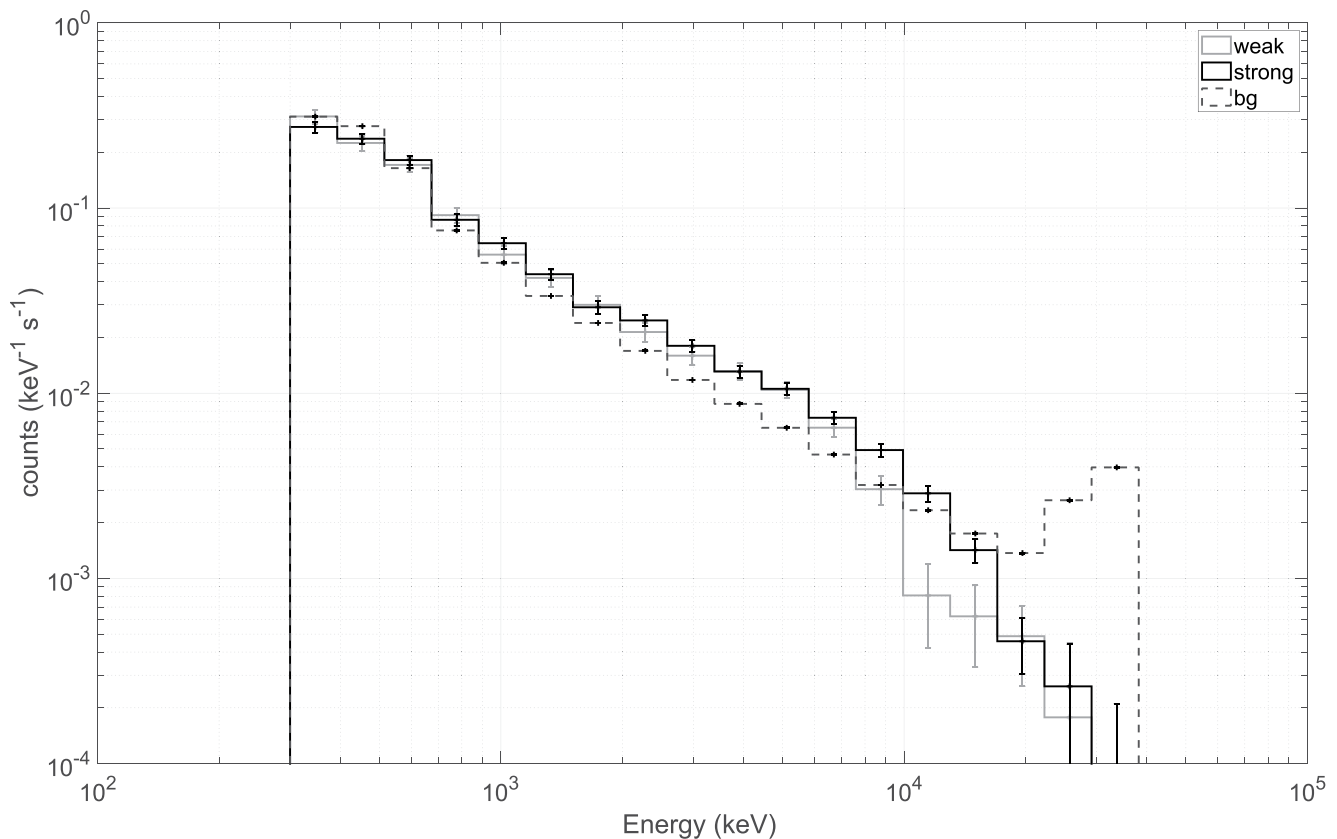


Figure 9. The background (dotted line) and the background-subtracted spectra (solid lines) of the strong and the weak flux enhancements. All spectra are normalized on their total intensity and duration. For the background spectra, the error bars are estimated as the square root of the number of counts in each bin. The background standard deviation σ is added to the error of the weak and the strong glow spectra in quadrature.

during the flux reduction moment in the vicinity of the aircraft. The clusters belong to one extensive hybrid IC/CG lightning.

The lightning started in a remote location from the aircraft with IC strokes in clusters 2 and 3, then progressed to cluster 1 located underneath the aircraft. It discharged a pocket charge region associated with the cluster 1 that caused the rapid glow flux reduction. The specific process that discharged the region was not particularly prominent neither in radio nor in optical emission. Moreover, we have not detected any extraordinarily large charge transfer during the flux reduction period but around it. We suggest that the most likely explanation to the discharge activity in cluster 1 is a positive leader propagation. The positive leader remains undetected in COLMA data and the LF antenna, it is barely seen in the HF antenna but showed some activity in the FEGS optical instrument. It is usually assumed that a bidirectional leader propagates symmetrically on both ends, positive and negative. During the flux reduction moment, the negative leader becomes very active in cluster 3, while the positive leader discharges the negative charge pocket of cluster 1. The observation is remarkably similar to what was reported in Wada et al. (2018).

We suggested that the observed periods of the weak and the strong flux enhancements may correspond to different glow production mechanisms. However, the spectral analysis did not confirm this. Both spectra were found to be similar to each other and to background with minor discrepancy. In the observation by Kelley et al. (2015), a gamma-ray glow had a several times higher count-rate at the peak than a background level, and therefore has been explained as produced by RREA mechanism. In the present case, the highest flux increase is only 43% higher than the background. Although the altitude of the aircraft is totally different, both glows presented here are probably caused by MOS mechanism rather than RREA. As has been demonstrated in Østgaard et al. (2019), the discussed, here, thundercloud had an inverted charge structure with an upper negative charge layer and a lower positive charge layer. In this situation, the observed

gamma-ray glows may have been produced between the upper negative charge layer and a screening layer of the thundercloud. Another two options for the glow production, a RREA inside the cloud and a cosmic-ray enhancement due to a decaying electric field above the cloud, were thoroughly modeled and discussed in Østgaard et al. (2019). In addition, a time-resolved analyses of the glow spectra did not show any significant change of the spectra in time and was not shown in the paper.

Data Availability Statement

The data used in this manuscript were uploaded to Zenodo repository (DOI <https://doi.org/10.5281/zenodo.3960321>). The optical data of the FECS instrument available on the NASA's website, the link is provided in the references.

Acknowledgments

This work was supported by the European Research Council under the European Union's Seventh Framework Program (FP7/2007–2013)/ERC grant agreement 320839 and the Research Council of Norway under contracts 208028/F50 and 223252/F50 (CoE). The authors thank the WWLLN and COLMA networks for the data. The authors thank Vaisala Inc. for access to the US National Lightning Detection Network data used in some analyses. The authors thank Earth Networks for providing the lightning data used in this study (<https://www.earthnetworks.com/>) and can be obtained by contacting Steve Prinzivalli (sprinzivalli@earthnetworks.com).

References

- Chilingarian, A., Daryan, A., Arakelyan, K., Hovhannisyian, A., Mailyan, B., Melkumyan, L., et al. (2010). Ground-based observations of thunderstorm-correlated fluxes of high-energy electrons, gamma rays, and neutrons. *Physical Review D*, 82(4), 043009. <https://doi.org/10.1103/physrevd.82.043009>
- Chilingarian, A., Mailyan, B., & Vanyan, L. (2012). Recovering of the energy spectra of electrons and gamma rays coming from the thunderclouds. *Atmospheric Research*, 114–115, 1–16. <https://doi.org/10.1016/j.atmosres.2012.05.008>
- Dwyer, J. R., Smith, D. M., Hazelton, B. J., Grefenstette, B. W., Kelley, N. A., Lowell, A. W., et al. (2015). Positron clouds within thunderstorms. *Journal of Plasma Physics*, 81(4). <https://doi.org/10.1017/s0022377815000549>
- Eack, K. B. (1996). Balloon-borne x-ray spectrometer for detection of x rays produced by thunderstorms. *Review of Scientific Instruments*, 67(5), 2005–2009. <https://doi.org/10.1063/1.1146959>
- Eack, K. B., & Beasley, W. H. (2015). Long-duration x-ray emissions observed in thunderstorms. *Journal of Geophysical Research: Atmospheres*, 120(14), 6887–6897. <https://doi.org/10.1002/2015jd023262>
- Eack, K. B., Beasley, W. H., Rust, W. D., Marshall, T. C., & Stolzenburg, M. (1996a). Initial results from simultaneous observation of X-rays and electric fields in a thunderstorm. *Journal of Geophysical Research*, 101(D23), 29637–29640. <https://doi.org/10.1029/96jd01705>
- Eack, K. B., Beasley, W. H., Rust, W. D., Marshall, T. C., & Stolzenburg, M. (1996b). X-ray pulses observed above a mesoscale convective system. *Geophysical Research Letters*, 23(21), 2915–2918. <https://doi.org/10.1029/96gl02570>
- Eack, K. B., Suszcynsky, D. M., Beasley, W. H., Roussel-Dupre, R., & Symbalisty, E. (2000). Gamma-ray emissions observed in a thunderstorm anvil. *Geophysical Research Letters*, 27(2), 185–188. <https://doi.org/10.1029/1999gl010849>
- Kelley, N. A., Smith, D. M., Dwyer, J. R., Splitt, M., Lazarus, S., Martinez-McKinney, F., et al. (2015). Relativistic electron avalanches in a thunderstorm discharge competing with lightning. *Nature Communications*, 6, 7845. <https://doi.org/10.1038/ncomms8845>
- Kochkin, P., Sarria, D., Skeie, C., Van Deursen, A. P., de Boer, A., Bardet, M., et al. (2018). In-flight observation of positron annihilation by ildas. *Journal of Geophysical Research: Atmospheres*, 123(15), 8074–8090.
- Kochkin, P., van Deursen, A., Marisaldi, M., Ursi, A., de Boer, A., Bardet, M., et al. (2017). In-flight observation of gamma ray glows by ILDAS. *Journal of Geophysical Research: Atmospheres*, 122(23). <https://doi.org/10.1002/2017jd027405>
- Marchand, M., Hilburn, K., & Miller, S. D. (2019). Geostationary lightning mapper and earth networks lightning detection over the contiguous United States and dependence on flash characteristics. *Journal of Geophysical Research: Atmospheres*, 124(21), 11552–11567. <https://doi.org/10.1029/2019JD031039>
- McCarthy, M., & Parks, G. (1985). Further observations of x-rays inside thunderstorms. *Geophysical Research Letters*, 12(6), 393–396. <https://doi.org/10.1029/GL012i006p00393>
- McGill, M., Hlavka, D., Hart, W., Scott, V. S., Spinhirne, J., & Schmid, B. (2002). Cloud physics lidar: Instrument description and initial measurement results. *Applied Optics*, 41(18), 3725–3734. <https://doi.org/10.1364/AO.41.003725>
- Østgaard, N., Christian, H. J., Grove, J. E., Sarria, D., Mezentsev, A., Kochkin, P., et al. (2019). Gamma ray glow observations at 20-km altitude. *Journal of Geophysical Research: Atmospheres*, 124(13), 7236–7254. <https://doi.org/10.1029/2019JD030312>
- Parks, G., Mauk, B., Spiger, R., & Chin, J. (1981). X-ray enhancements detected during thunderstorm and lightning activities. *Geophysical Research Letters*, 8(11), 1176–1179. <https://doi.org/10.1029/GL008i011p01176>
- Quick, M., Blakeslee, R. J., Christian, H., Jr, Stewart, M. F., Podgorny, S., & Corredor, D. (2015). Airborne GLM Simulator (FECS). *American Geophysical Union, fall meeting, 2015, GC33D–1316*.
- Quick, M. G., Christian, H., & Blakeslee, R. J. (2019). GOES-R PLT Fly's Eye GLM simulator (FECS). <http://doi.org/10.5067/GOESR-PLT/FECS/DATA101>, data retrieved from EARTHDATA in October 2019. Retrieved from <https://ghrc.nsstc.nasa.gov/hydro/details/goesrpltfecs>
- Rudlosky, S. D. (2015). Evaluating ENTLN performance relative to TRMM/LIS. *Journal of Operational Meteorology*, 3(2), 11–20.
- Stano, G. T., Szoke, E. J., Rydell, N., Cox, R., & Mazur, R. (2014). Colorado lightning mapping array collaborations.
- Tatum, P. (2017). NASA ER2 aircraft landing March 21, 2017. Retrieved from https://www.youtube.com/watch?v=inEQBAzWX_M
- Tsuchiya, H., Enoto, T., Iwata, K., Yamada, S., Yuasa, T., Kitaguchi, T., et al. (2013). Hardening and termination of long-duration γ rays detected prior to lightning. *Physical Review Letters*, 111(1). <https://doi.org/10.1103/PhysRevLett.111.015001>
- Wada, Y., Bowers, G. S., Enoto, T., Kamogawa, M., Nakamura, Y., Morimoto, T., et al. (2018). Termination of electron acceleration in thundercloud by intracloud/intercloud discharge. *Geophysical Research Letters*, 45(11), 5700–5707. <https://doi.org/10.1029/2018GL077784>
- Wada, Y., Enoto, T., Nakamura, Y., Furuta, Y., Yuasa, T., Nakazawa, K., et al. (2019). Gamma-ray glow preceding downward terrestrial gamma-ray flash. *Communications Physics*, 2(1), 67. <https://doi.org/10.1038/s42005-019-0168-y>
- Zhu, Y., Rakov, V., Tran, M., Stock, M., Heckman, S., Liu, C., et al. (2017). Evaluation of ENTLN performance characteristics based on the ground truth natural and rocket-triggered lightning data acquired in Florida. *Journal of Geophysical Research: Atmospheres*, 122(18), 9858–9866. <https://doi.org/10.1002/2017JD027270>